

Wet-Chemical Synthesis of Surface Passivated Halide Perovskite Microwires for Improved Optoelectronic Performance and Stability

*Qian Ye^{a,b} ‡, Jin Zhang^a ‡, Pengfei Guo^a, Haibo Fan^c, *, Dmitry Shchukin^{d,e}, Bingqing Wei^{a,e,f},
Hongqiang Wang^{a,e},*

^aState Key Laboratory of Solidification Processing, Center for Nano Energy Materials, School of Materials Science and Engineering, Northwestern Polytechnical University and Shaanxi Joint Laboratory of Graphene (NPU), Xi'an, 710072, P. R. China.

^bResearch & Development Institute of Northwestern Polytechnical University in Shenzhen, Xi'an, 710072, P. R. China

^cSchool of Physics, Northwest University, Xi'an, 710069, P.R. China

^dStephenson Institute for Renewable Energy, Department of Chemistry, University of Liverpool, Crown Street, Liverpool, L69 7ZD, United Kingdom

^eNPU-UoL International Joint Lab of Advanced Nanomaterials for Energy Applications, Xi'an, 710072, P. R. China

^fDepartment of Mechanical Engineering, University of Delaware, Newark, Delaware 19716 ,
United States.

KEYWORDS: Perovskite Microwires, PFA, Surface Passivation, Photodetector, Stability

ABSTRACT

1D halide perovskite materials with intrinsic high carrier mobility and long diffusion length hold great promises for high-performance optoelectronic devices, in which the passivation of the surface defects is of significance for further boosting its optoelectronic performance as well as its moisture stability. Herein, we demonstrate a simple room temperature wet-chemical synthetic protocol for perovskite microwires with controlled morphologies and passivated surface states. This strategy allows for facile assembly of hydrophobic 1H,1H-perfluorooctylamine (PFA) molecule on the surface of the perovskite microwires owing to the coordination binding between the amino groups of PFA and Pb^{2+} . Both steady and time resolved photoluminescence measurements revealed the passivation of PFA greatly benefit for the inhibition of the photogenerated carriers recombination. The constructed perovskite microwires based photodetectors have shown increased detectivity of 4.99×10^{11} Jones and responsivity of 1.27 A/W (light power density of 1 mW/cm^2). Moreover, the hydrophobic fluorocarbon alkyl chains endow the perovskite microwires with higher resistance towards moisture. Such coating of a water-resisting layer resulted in greatly enhanced stability of perovskite microwires under the humidity of $55 \pm 5\%$ over 30 days. We thus believe that our work is of importance for the

development of 1D halide perovskite photodetectors with highly improved performance and stability.

Introduction

Organic-inorganic hybrid perovskites have recently attracted increasing research interests as the potential candidates for optical and electrical devices, such as photovoltaics,¹⁻³ light-emitting diodes,⁴ lasers⁵ and photodetectors,⁶⁻⁸ due to their long diffusion length, direct energy bandgap, and good optical absorption property.⁹ For these optoelectronic applications, the microstructures and crystalline quality of the perovskite materials play key roles for the device performance.⁶ From two-dimensional (2D) polycrystalline films and nanosheets,¹⁰ one-dimensional (1D) nanowires (NWs),¹¹⁻¹⁴ to zero-dimensional quantum dots,¹⁵ versatile perovskite crystals have been explored for high-performance devices. Compared to the other morphologies of the perovskite, 1D NWs exhibit the advantages of higher carriers mobility and longer diffusion length,⁶ which make 1D perovskite nanostructures very promising as building blocks for the optoelectronic applications. However, as an ionic material, the 1D perovskite crystal also has a reasonable quantity of non-coordinated ions, which are likely to form defects both on the surface and grain boundaries (GBs).¹⁶ These defects would reduce device performance due to their negative effects on carrier lifetime and transportation, as evidenced by the much longer measured photoluminescence recombination lifetime after reducing the defect concentrations.¹ In addition, it has been recently reported that the decomposition of perovskite is always from the location of these defects, where ions are more active and more vulnerable to moisture and oxygen erosion.¹⁷ The instability of the 1D perovskite nanostructure is a key issue that has to be tackled for long-lived perovskite photodetectors, especially when compared with highly stable inorganic

semiconductors. Therefore, the synthesis of high quality perovskite with decreased surface and GBs defect intensities favors for not only the enhancement of the performance but also the improvement of the moisture durability.

Thanks to the great efforts devoted to the design of 1D $\text{CH}_3\text{NH}_3\text{PbI}_3$ perovskite nanostructures, a series of well aligned and single-crystalline $\text{CH}_3\text{NH}_3\text{PbI}_3$ NWs have been fabricated with high crystallographic order and decreased GBs,^{6, 11} which could serve as recombination centers especially in polycrystalline perovskite nanostructures. However, GBs have been reported by several recent studies to be inert toward charge recombination, and favoring for the separation of charge carriers.¹⁸ In this regard, surface passivation holds more promises for further improving the performance and durability of 1D $\text{CH}_3\text{NH}_3\text{PbI}_3$ perovskite nanostructures. Comparing to the well-studied surface passivation strategies and diverse passivation agents such as Lewis acid-base adduct adopted for perovskite solar cells,¹⁹⁻²¹ there have been very few reports on improving 1D perovskite photodetectors performance based on surface passivations²². Therefore, there is a great need for developing synthetic methods that allow for well controlled 1D nanostructure growth as well as the surface defects passivation.

Herein, inspired by one of the rarely reported work of surface passivation for enhanced photocurrent density and improved stability by using oleic acid soaking,²² we demonstrate a simple but effective surface passivation protocol by using PFA as a novel passivation agent. Comparing to the reported passivant of oleic acid, PFA bears the advantages of being as electron acceptors that could bind better to the defects of organic perovskites, as well as its unique molecular structure (amino and C-F groups) favoring for defect passivation and hydrophobic barrier. Such reactive molecule is expected to perform in a bifunctional manner to improve the as-formed perovskite microwires. On the one hand, the lone pair electrons at the amino groups

can form coordination bonds by delocalizing to 6p empty orbitals of Pb^{2+} to possibly passivate perovskite microwires surface defects,²³ on the other hand, the hydrophobic fluorocarbon alkyl chains can endow the perovskite microwires with higher resistance towards moisture. Moreover, the presented facile room temperature wet-chemical synthetic method allows for the controlled morphologies and passivated surface states of the resulted perovskite microwires. Our study revealed that PFA passivated microwires show extended carrier lifetime, and increased carrier mobility, resulting in enhanced responsivity, detectivity and long-term stability of the as-prepared photodetectors. We thus believe that our work is useful for developing high performance 1D halide perovskite based photodetectors by exploring surface passivation protocols.

Experimental Section

Materials

PbI_2 (99.99%), PbCl_2 (99.99%) and Methyl Amine Iodide (MAI) (99.99%) were ordered from Xi'an Polymer Light Technology Corp. Super dehydrated isopropanol (IPA) and *N,N*-Dimethylformamide (DMF) were ordered from Sigma Aldrich. PFA was purchased from Energy Chemical.

Synthesis and Characterization of $\text{CH}_3\text{NH}_3\text{PbI}_3$ Microwires

PbI_2 powder (461.1 mg) was added into 1mL DMF solvent. Then it was heated to 70 °C in hot plate for 1h. The MAI (159 mg) was added into 20mL IPA solution and vigorously stirred at room temperature for 30 min under protection of argon. After that, the PbI_2 solution was gradually added into $\text{CH}_3\text{NH}_3\text{I}$ in IPA solution and it was violently shaken with stirring for 30

min still under argon atmosphere. For the reference $\text{CH}_3\text{NH}_3\text{PbI}_3$, the concentration of PbI_2 was 0 (PbI_2 powder with no DMF directly added into MAI solution in IPA), 2M, and 0.5M, respectively. For the preparation of $\text{CH}_3\text{NH}_3\text{PbI}_x\text{Cl}_{3-x}$ microwires, PbCl_2 powder (834 mg) is added into 1mL DMF. The PFA modified perovskite microwires were obtained by adding different concentration of PFA (2.5%, 5% and 10%, respectively) after formation of the perovskite microwires and stirring for 30 minutes.

Fabrication of Photodetectors

Glass substrates (size $1.5 \times 1.5 \text{cm}^2$) were rinsed respectively with deionized water, acetone and ethanol for 20 minutes, and dried with nitrogen. Before device fabrication, the FTO glasses were treated in a plasma cleaner for 10 min. The $\text{CH}_3\text{NH}_3\text{PbI}_3$ precursor solution were spin coated on FTO substrate with 1000 rpm for 20 s then spin rate accelerated up to 2000 rpm for 20 s, and repeated spin coating 10 times until the substrate is completely covered. The substrates were transferred to hot plate and heated at 100°C for 5 min between each spin coating. $\text{CH}_3\text{NH}_3\text{PbI}_3$ microwires were then coated by a layer of Au electrode (200 nm) that was deposited by e-beam evaporation (Kurt J Lesker Company, PVD 75). The size of the device channel, e.g. length and width was confirmed to be 1 mm and $60 \mu\text{m}$, respectively.

Characterization

The morphology was investigated on Scanning Electron Microscopy (SEM, FEI, Model Quanta 200 FEG), Transmission Electron Microscopy (TEM, FEI, Model Tecnai G2F20). X-ray Diffraction (XRD) pattern was recorded on a PANalytical X'pert PRO. UV-Vis-NIR diffuse reflectance spectrum for perovskite films were recorded using a UV-Vis-NIR spectrophotometer (PerkinElmer Lambda 950). The PL spectra were analyzed using a fluorescence

spectrophotometer (F-4600, Tokyo, Japan). X-ray photoelectron spectroscopy (XPS) data was collected on a PHI VersaProbe II XPS system and the C1s line at 284.6 eV were used as the reference for the binding energies of the other elements' orbitals from adventitious carbon.

Photodetectors Measurement.

The optoelectronic performance of the photodetector was measured by a semiconductor characterization system (Keithley 2400 source meter) under different bias voltages and light illumination densities. A Lake Shore Hall test system (7700A) was used to measure the carrier concentration and carrier mobility of the microwires.

Results and discussion

In this work, 1D $\text{CH}_3\text{NH}_3\text{PbI}_3$ microwires were prepared via a simple wet-chemical synthesis. Experimentally, PbI_2 in DMF solution was added directly into the IPA solution of $\text{CH}_3\text{NH}_3\text{I}$, as shown in **Figure 1a**. By simply stirring for several tens of minutes, a faint yellow stable solution could be obtained (**Figure 1b**). It is clear that the products have formed 1D structures in IPA through optical microscope images (**Figure S1**). The scanning electron microscope (SEM) image of perovskite microwires dispersed on silicon wafers after solvent completely evaporated are shown in **Figure 1c**, revealing that the $\text{CH}_3\text{NH}_3\text{PbI}_3$ microwires have a uniform width of 0.6-2 μm and aspect ratio of about 200 (**Figure S2**). This is agreement with the result of the TEM image of the perovskites (**Figure 1d**). The crystal structure of $\text{CH}_3\text{NH}_3\text{PbI}_3$ microwires is examined by XRD and high-resolution TEM (HRTEM). **Figure 1f** shows the XRD pattern of the $\text{CH}_3\text{NH}_3\text{PbI}_3$ microwires. The major diffraction peak at 14.34° and 28.68° are corresponding to the (110) and (220) crystal planes, indicating that it is preferable orientated along the [110] direction, similar as reported in the previous literature.⁷ The typical crystal plane of (220) with

the lattice distance of 0.33 nm shown in the HRTEM image (**Figure 1e**) further reveals the tetragonal phase of the $\text{CH}_3\text{NH}_3\text{PbI}_3$ microwire and the preferential growth direction along [220]. UV-Vis absorption (**Figure 1g**) is employed to investigate the optical properties of the $\text{CH}_3\text{NH}_3\text{PbI}_3$ microwires, where the absorption edge locates at 750 nm, corresponding to the band gap of 1.65 eV. The above results collectively show that high-quality $\text{CH}_3\text{NH}_3\text{PbI}_3$ microwires have been successfully fabricated.

To systematically investigate the kinetics of the perovskite microwires growth, different concentrations of PbI_2 of DMF (0, 0.5M, 1M and 2M) were dropped into the MAI/IPA solution. According to the SEM images, we can see that the products are perovskite particles rather than microwires when PbI_2 are directly added into the IPA without any DMF (**Figure 2a**). Mixture of fused particles and microwires are formed at the same time by adding 2M PbI_2 (**Figure 2b**), while microwires can be formed when decrease the PbI_2 concentration to 1M (**Figure 2c**). When the PbI_2 concentration is 0.5M, the diameter and length of the microwires will be increased and decreased upon adding more DMF, respectively (**Figure 2d**). In addition, we also prepare 1D $\text{CH}_3\text{NH}_3\text{PbI}_x\text{Cl}_{3-x}$ microwires structure with smaller diameter (**Figure 2e**) due to the larger molecular volume of pure $\text{CH}_3\text{NH}_3\text{PbI}_3$ ²⁴⁻²⁵. As discussed above, it is obvious that DMF plays a decisive role in the formation of perovskite microwires, so we studied the effect of DMF on PbI_2 . Interestingly, we found that the remaining PbI_2 was in a 1D structure when DMF is completely volatile from saturated PbI_2 solution, as shown in **Figure 2f**. It is reported that PbI_2 could form coordination bonding at its edge of (002) plane with DMF.²⁶ We thus postulate that MAI is combined with that exposed plane of PbI_2 and grows along the vertical crystal orientation to form an anisotropic perovskite microwires. The presence of microparticles is due to the fact that a smaller amount of DMF does not cause the plane face of PbI_2 to be completely exposed. The

different concentrations of MAI in of IPA (0.025M, 0.05M and 0.1M) were also studied in our experiment. According to the SEM images in **Figure S3**, the concentrations of MAI in of IPA have no significant effect on the formation of perovskite wires.

As mentioned above, the surface defects and the hydrophilic nature of the 1D perovskite seriously hindered its application for high performance optoelectric devices, so we intended to introduce a surface passivation layer on the perovskite microwires to alleviate these obstacles. **Figure 3a** shows the process of adding PFA by adding an appropriate amount of PFA after formation of the perovskite microwires and stirring for a few more minutes. The PFA modified $\text{CH}_3\text{NH}_3\text{PbI}_3$ microwires are characterized by the XPS spectrum (**Figure 3b**), which demonstrates the existing of C, N, O, Pb, I and F. Successful PFA modification is indicated by the presence of F1s binding energy at 686.96 eV which is not detected for the untreated $\text{CH}_3\text{NH}_3\text{PbI}_3$ microwires. The XRD pattern in **Figure 3c** indicates that the crystalline had little change after PFA modification. Adding PFA caused also no obvious change in morphology, indicated by the clean and smooth surface of the PFA modified perovskite microwires, as seen from the SEM images in **Figure S4**. The wettability behavior of the PFA modified perovskite microwires could be characterized by contact angle measurements. The perovskite microwires has a lower contact angle (CA) values of 65.8° , but the CAs of PFA modified perovskite microwires is 88.7° (**Figure S5**).

However, the PL intensities are obviously enhanced after PFA modification (**Figure 4a**), indicating that photo-generated carrier radiation recombination increased. In other word, the non-radiative carrier recombination of the as-prepared $\text{CH}_3\text{NH}_3\text{PbI}_3$ microwires were effectively inhibited after PFA modification owing to the decreased trap states, which is beneficial to the optoelectric applications. We thus fabricated photodetectors of the perovskite microwires by

depositing gold (Au) electrodes onto the $\text{CH}_3\text{NH}_3\text{PbI}_3$ microwires through a shadow mask (**Figure 4b**). Each electrode have a width of about $40\mu\text{m}$, a length of 1mm and an effective illuminated area of 0.12 mm^2 . Its spectral responsivity is measured to study the device response to different input optical wavelengths (**Figure 4c**). The responsivity (R) of a photodetector, is defined as $R = \Delta I/PA$, where ΔI depicts the gap between the photocurrent and the dark current ($\Delta I = I_{\text{light}} - I_{\text{dark}}$), P is the light power intensity, and A is the illuminated area of the photodetector.²⁷ The responsivity of PFA modified $\text{CH}_3\text{NH}_3\text{PbI}_3$ microwires is calculated to be 0.25 A/W from 450 nm to 780 nm . It can be seen that the device has a consistent photoelectric response in the range of the optical absorption of the as-prepared $\text{CH}_3\text{NH}_3\text{PbI}_3$ microwires. Meanwhile, we find that the responsivity of PFA modified devices are higher than those without PFA (0.21A/W), which confirms that PFA has an positive influence on the photoelectric properties of the detector.

To further explore the optimized impact of PFA on the optoelectric properties, the different concentrations of PFA (The molar ratio of PFA/ PbI_2 was 0, 2.5%, 5% and 10% respectively) are used during preparation, while the other conditions are kept the same. According to the I-t curves in **Figure S6**, the photocurrent reached the maximum when adding 5% PFA, which is found as an optimal concentration for perovskite microwires modification and the next characterizations are all carried out at this condition. This may be because too much PFA will reduce the carrier mobility, and less PFA cannot fully passivate the surface defects of the $\text{CH}_3\text{NH}_3\text{PbI}_3$ microwires. Higher amount of PFA can deduce phase separation between MAPbI_3 and PFA molecules, thus hindering the charge transportation.

The current-voltage (I-V) curves of the PFA modified microwires based photodetectors are demonstrated in **Figure 4d** under light and dark conditions from 0 V to 1 V bias. The

photocurrent to dark current ratio ($I_{\text{light}}/I_{\text{dark}}$), which depicts the switching ratio of a photodetector, reached higher than 250 at 1V bias for the modified microwires based photodetectors, owing to the increased light current and slightly decreased dark current. As showed in **Figure S7**, the dark current for PFA passivation devices is only several pA. The current-time (I-t) curves (**Figure 4e**) were collected using a light-emitting diode (LED) laser emitting at 525 nm (power intensity of 3 mW/cm²). It can be observed that the photocurrent of the device with PFA increased more than twice compared to that of without passivation.

The spectral responsivity and detectivity (D^*) were also measured. The detectivity can be defined by the equation of $D^* = \frac{\Delta I \sqrt{A}}{P \sqrt{2qI_d}}$, where q is elementary charge, R is responsivity, A is device area, B is electrical bandwidth, and I_n is noise current.²⁷ **Figure 4f** shows the R and D^* for detectors based on both the $\text{CH}_3\text{NH}_3\text{PbI}_3$ microwires with PFA at a fixed bias of 1 V. It can be seen that as the current density increases, both R and D are reduced nearly linearly, due to enhanced exciton combination at high carrier concentration. At the light power intensity of 1 mW/cm² intensity, the specific detectivity of PFA modified perovskite microwires can reach 4.99×10^{11} Jones, and the responsivity can reach 1.27 A/W, which is higher than the responsivity of unmodified device (0.57A/W), as shown in **Figure S8**. The increase is attributable to the longer carrier lifetime, higher carrier mobility and reduced charge trap density of the microwires after passivation by PFA.

The time resolved photoluminescence (TRPL) measurements are adopted to clarify the influence of PFA modification on $\text{CH}_3\text{NH}_3\text{PbI}_3$ surface defects. **Figure 4g** shows the TRPL curves of $\text{CH}_3\text{NH}_3\text{PbI}_3$ microwires prepared on glass substrates with/without modification with PFA. TRPL traces can be fitted by a biexponential profiles, where the fast decay process

corresponds to the quenching of surface recombination while the slow decay correlates with radiative decay in bulk component.³ The fast and slow component of PL lifetime of PFA modified CH₃NH₃PbI₃ microwires can be extracted as $\tau_1=48.12$ ns and $\tau_2=13.52$ ns, noticeably larger than that of $\tau_1=19.43$ ns and $\tau_2=4.14$ ns for bare CH₃NH₃PbI₃ microwires. This result suggests that non-radiative recombination of CH₃NH₃PbI₃ microwires is suppressed by the PFA passivation.

The trap-state density was measured by the I-V response of crystals and space charge limited current (SCLC) analysis, as shown in **Figure 4h-i**. The charge-trap density, n , can be given by $n=2\varepsilon\varepsilon_0VTEL/qd^2$ gives, where ε and ε_0 is the relative and absolute vacuum dielectric constants, respectively, and d is the length of the conductive channel. Charge-trap density of 4.69×10^8 cm⁻³ is measured for PFA modified CH₃NH₃PbI₃ microwires, which is much lower than that of 3.93×10^9 cm⁻³ for bare CH₃NH₃PbI₃ microwires. Meanwhile, carrier concentration and mobility can also be calculated according to the corresponding formula. Mobility of PFA-passivated CH₃NH₃PbI₃ microwires increases from 1.04 cm²/(V s) to 1.18 cm²/(V s), and the carrier density decrease to 2.65×10^8 cm⁻³ from 1.65×10^9 cm⁻³. Therefore, the dark current of PFA-passivated devices becomes lower owing to the decreased carrier density, and the enhanced photocurrent is because of the increased mobility and carrier lifetime.

Moisture durability is of significance for perovskite photodetector owing to that perovskite materials are fragile and susceptible to decomposition by various factors. Figure 5 shows the results of stability tests of the corresponding perovskite microwires in ambient condition (55% \pm 5% relative humidity) without encapsulation. It is clear from these characterizations that the PFA modification of microwires-based film provides better stability than that of the control film. For example, as shown in **Figure 5a**, the microwires-based film without PFA modification changed

to clear yellow within 20 days, while the modified film has no significant color change. The XRD analysis shown in **Figure 5b** indicates that a new phase that can be indexed to PbI_2 appeared, for the microwires-based film without PFA modification after 20 days exposure in humidity chamber. In contrast, for the PFA modified $\text{CH}_3\text{NH}_3\text{PbI}_3$ microwires, the PbI_2 peak is almost invisible, implying the PFA modification perovskite film presenting substantial increase in stability. To find the origin of the improved moisture-resistance, we studied the chemical structure of the PFA and its interaction with perovskite, as shown in **Figure 5c**. PFA is characterized by the presence of an amino group capable of coordinating with perovskite and numerous C-F functional groups. It has been recently reported that the defect sites where there are plenty of active defects favors generally for the initialization of the perovskite degradation.¹⁷ Thus, we speculate that the interaction between PFA and $\text{CH}_3\text{NH}_3\text{PbI}_3$ can improve the microwires' stability owing to the passivation of these defects on the perovskite surface. What's more, the fluorocarbon chains make the material to be extremely hydrophobic. The photocurrent of the photodetectors based on unmodified perovskite degraded to <60% after 30 days (humidity: $60\pm 5\%$; temperature, 298 K). In contrast, the photocurrent value of the PFA modified perovskite photodetectors remained above 80% under the same condition (**Figure S9**). Hence, through this method, an improved moisture stability of the $\text{CH}_3\text{NH}_3\text{PbI}_3$ microwires can be easily achieved.

Conclusion

In summary, we have demonstrated a simple synthetic route for 1D perovskite microwires with tunable morphologies and compositions by controlling the experimental parameters. A novel passivation agent of PFA can be easily assembled on the surfaces of the 1D perovskite microwires. Our results indicated that the PFA passivation could result in prolonged carrier lifetime, improved carrier mobility and decreased trap density of the resulted 1D perovskite

microwires. As a result, the photodetectors based on the PFA passivated 1D perovskite microwires demonstrated increased detectivity of 4.99×10^{11} Jones and responsivity of 1.27 A/W, which is much higher than those of the devices based on $\text{CH}_3\text{NH}_3\text{PbI}_3$ microwires without modification. The hydrophobic fluorocarbon alkyl chains make the surface of the perovskite more resistant to moisture. The greatly improved carrier mobility and reduced defect density, as well as the enhanced photodetector performance and stability achieved in present work via small molecular passivation, is of great significance for exploring 1D perovskite based photodetectors with highly improved performance and stability.

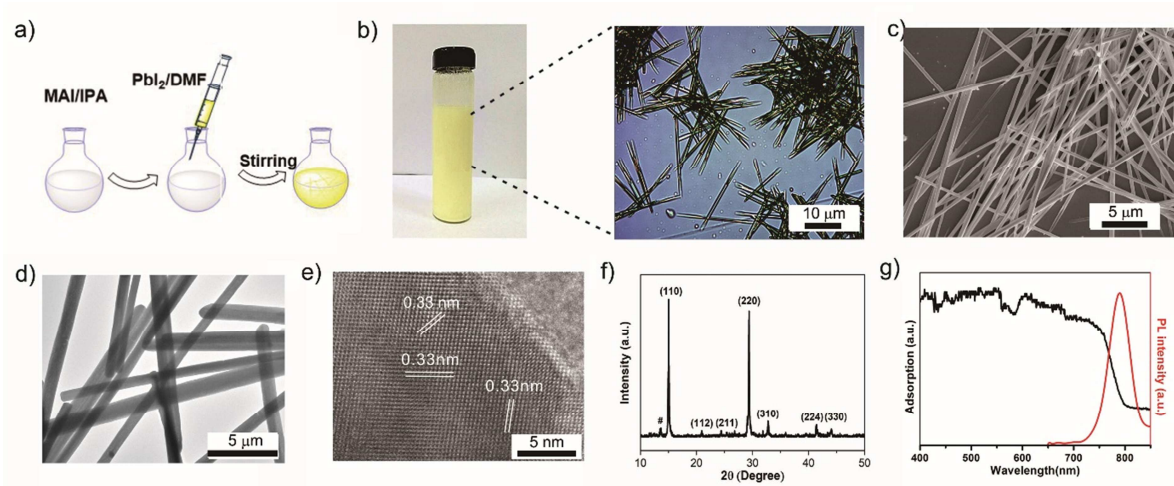


Figure 1. Characterization of $\text{CH}_3\text{NH}_3\text{PbI}_3$ microwires. a) Schematic illustration of the fabrication procedure, b) Optic microscope image in the solvent of IPA, c) Top-view SEM image, d) TEM image, e) HR-TEM image, f) XRD pattern, and g) UV-Vis and PL spectra.

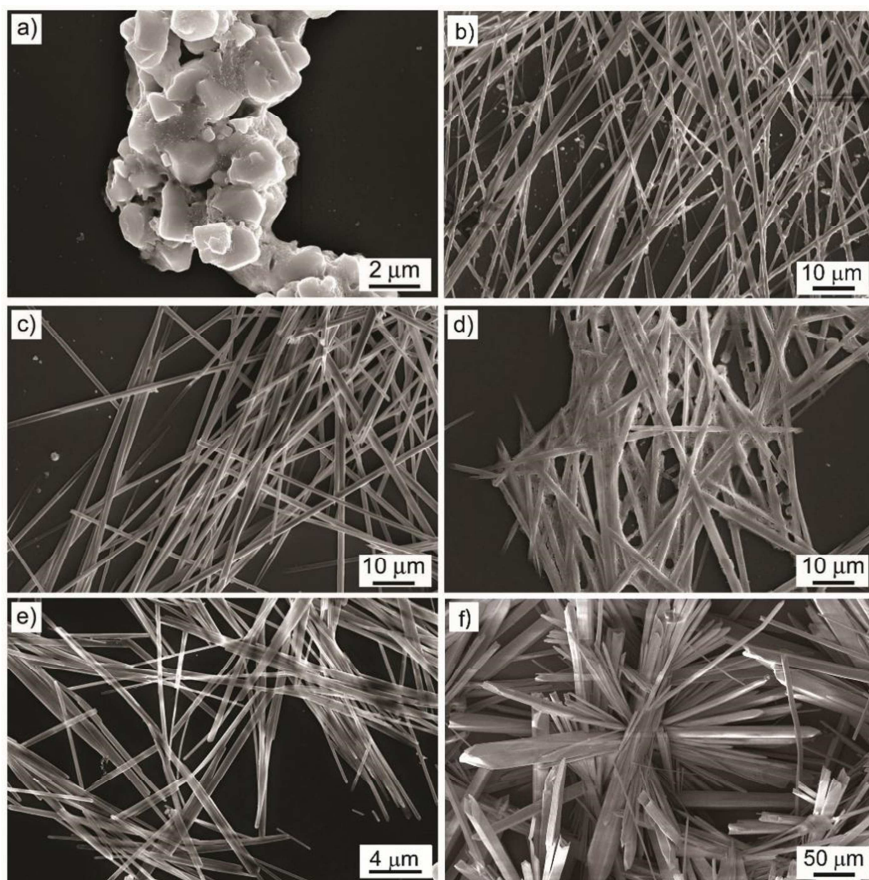


Figure 2. SEM images of the products obtained a) without adding DMF, and via changing concentrations of PbI_2 in DMF: b) 2 M, c) 1 M and d) 0.5 M. SEM images of e) $\text{CH}_3\text{NH}_3\text{PbI}_x\text{Cl}_{3-x}$ microwires and f) PbI_2 after DMF completely volatilized.

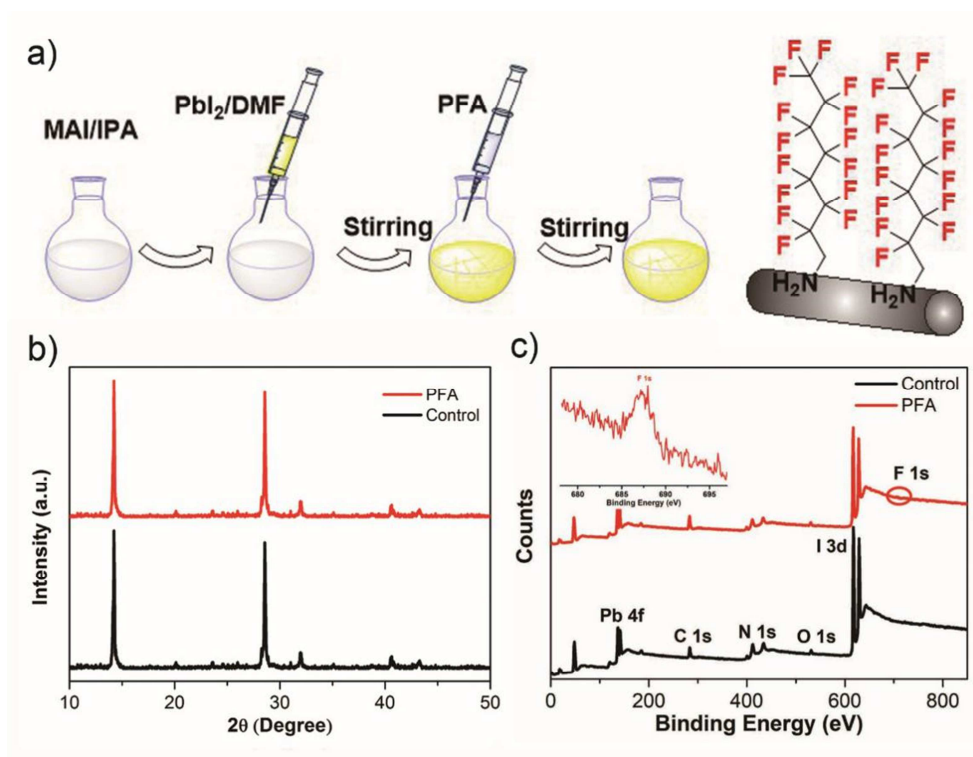


Figure 3. a) Schematic illustration of the experimental preparation of PFA modified $\text{CH}_3\text{NH}_3\text{PbI}_3$ microwires, b) XRD analysis and c) XPS survey spectra of control and PFA modified $\text{CH}_3\text{NH}_3\text{PbI}_3$ microwires.

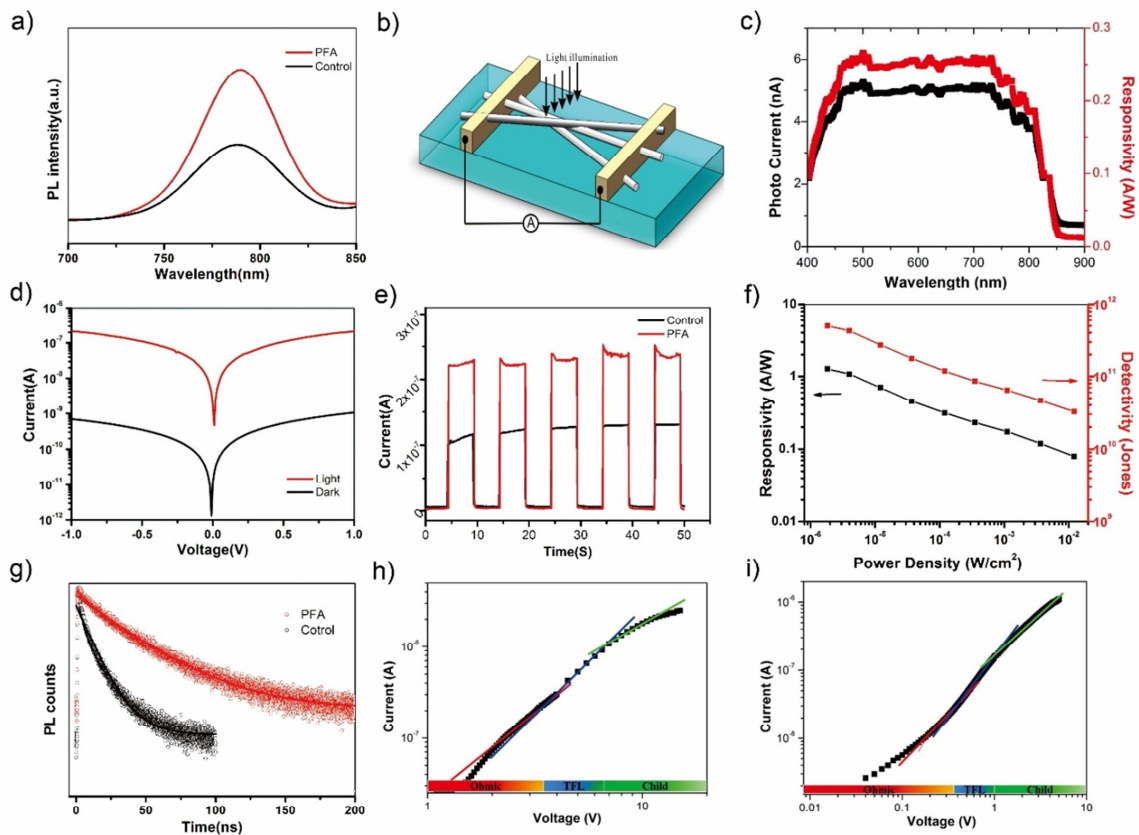


Figure 4. a) PL spectra of $\text{CH}_3\text{NH}_3\text{PbI}_3$ microwires with and without PFA modification, b) Schematic depiction of the device structure of the microwires based photodetector, c) Evolution of photocurrent and responsivity of $\text{CH}_3\text{NH}_3\text{PbI}_3$ microwires upon wavelength, d) IV curves of the PFA modified $\text{CH}_3\text{NH}_3\text{PbI}_3$ microwires, e) Transient photoresponses, f) Evolution of responsivity and detectivity upon light intensity, g) Decay transient of $\text{CH}_3\text{NH}_3\text{PbI}_3$ microwires with and without PFA passivation. SCLC characterizations of $\text{CH}_3\text{NH}_3\text{PbI}_3$ microwires h) without PFA modification and i) with PFA modification.

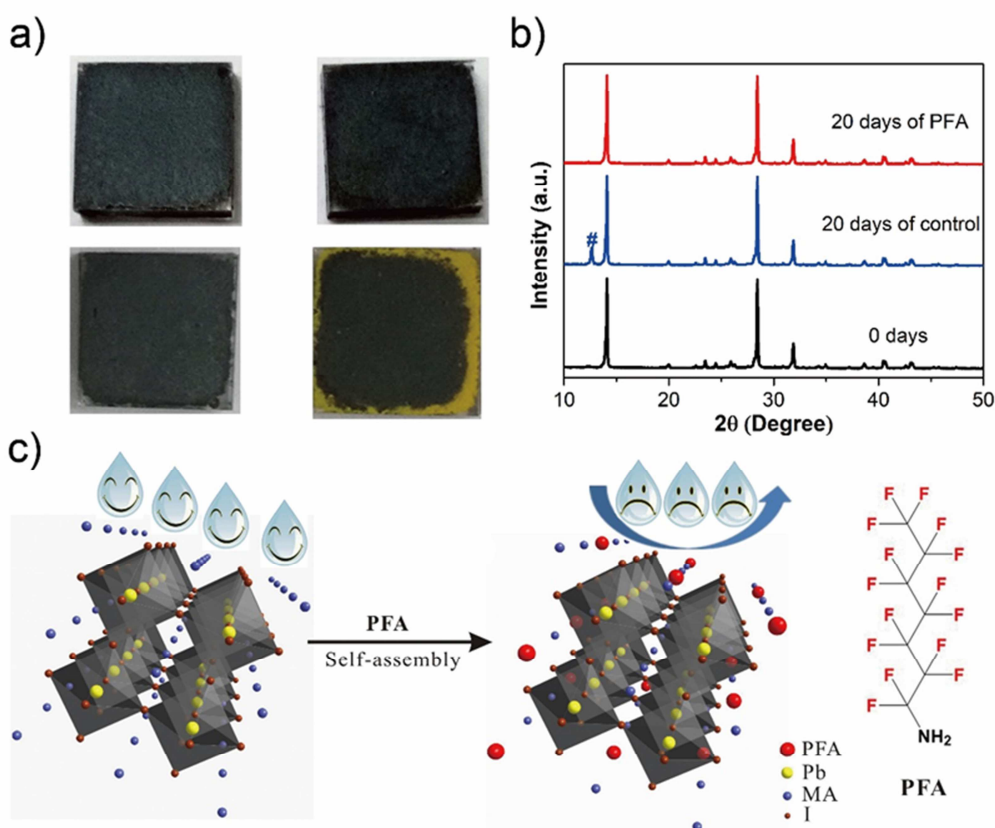


Figure 5. a) Photographic images of original $\text{CH}_3\text{NH}_3\text{PbI}_3$ microwires (right top), PFA modified $\text{CH}_3\text{NH}_3\text{PbI}_3$ microwires films (left top), $\text{CH}_3\text{NH}_3\text{PbI}_3$ microwires in humidity for 30 days (right bottom) and PFA modified $\text{CH}_3\text{NH}_3\text{PbI}_3$ microwires films in humidity for 30 days (left bottom), b) XRD patterns of $\text{CH}_3\text{NH}_3\text{PbI}_3$ microwires without and with 5 % PFA passivation, in ambient condition with a relatively humidity of 55% and c) Schematic illustration of the chemical structure of the PFA and its interaction with perovskite.

ASSOCIATED CONTENT

Supporting Information. The Supporting Information is available free of charge on the ACS Publications website at DOI: Optic microscope images of $\text{CH}_3\text{NH}_3\text{PbI}_3$ microwires in IPA at

different stage; the SEM images and size distribution of perovskite microwires; Transient photoresponses of $\text{CH}_3\text{NH}_3\text{PbI}_3$ microwires with different concentrations of PFA; the wettability behavior and Light-dark current-voltage (I-V) curves of control and PFA modified microwires, the responsivity of photodetectors based on control and PFA modified microwires.

AUTHOR INFORMATION

Corresponding Author

*E-mail: hbfan@nwu.edu.cn (Haibo Fan), hongqiang.wang@nwpu.edu.cn (Hongqiang Wang)

Author Contributions

The manuscript was written through contributions of all authors. All authors have given approval to the final version of the manuscript. ‡These authors contributed equally.

Notes

Any additional relevant notes should be placed here.

ACKNOWLEDGMENT

This work was financially support by NSFC (51672225), Science and Technology Program of Shenzhen (JCYJ20170306153027078), Natural Science Foundation of Shaanxi (2017JM5028, 2017JM2013, 2017JM1030), the Fundamental Research Funds for the Central Universities (G2017KY0002) and the 1000 Youth Talent Program of China. We would like to thank the Analytical & Testing Center of Northwestern Polytechnical University for analyzing structure and performance of the as-prepared materials.

REFERENCES

- (1) Zheng, X.; Chen, B.; Dai, J.; Fang, Y.; Bai, Y.; Lin, Y.; Wei, H.; Zeng, Xiao C.; Huang, J. Defect passivation in hybrid perovskite solar cells using quaternary ammonium halide anions and cations. *Nat. Energy* **2017**, *2* (7), 17102.
- (2) Zhang, J.; Hu, Z.; Huang, L.; Yue, G.; Liu, J.; Lu, X.; Hu, Z.; Shang, M.; Han, L.; Zhu, Y. Bifunctional alkyl chain barriers for efficient perovskite solar cells. *Chem. Commun.* **2015**, *51* (32), 7047-7050.
- (3) Son, D. Y.; Lee, J. W.; Choi, Y. J.; Jang, I. H.; Lee, S.; Yoo, P. J.; Shin, H.; Ahn, N.; Choi, M.; Kim, D.; Park, N. G. Self-formed grain boundary healing layer for highly efficient CH₃NH₃PbI₃ perovskite solar cells. *Nat. Energy* **2016**, *1* (7), 16081.
- (4) Tan, Z. K.; Moghaddam, R. S.; Lai, M. L.; Docampo, P.; Higler, R.; Deschler, F.; Price, M.; Sadhanala, A.; Pazos, L. M.; Credgington, D.; Hanusch, F.; Bein, T.; Snaith, H. J.; Friend, R. H. Bright light-emitting diodes based on organometal halide perovskite. *Nat. Nanotechnol* **2014**, *9* (9), 687-692.
- (5) Liao, Q.; Hu, K.; Zhang, H.; Wang, X.; Yao, J.; Fu, H. Perovskite Microdisk Microlasers Self-Assembled from Solution. *Adv. Mater.* **2015**, *27* (22), 3405-3410.
- (6) Feng, J.; Yan, X.; Liu, Y.; Gao, H.; Wu, Y.; Su, B.; Jiang, L. Crystallographically Aligned Perovskite Structures for High-Performance Polarization-Sensitive Photodetectors. *Adv. Mater.* **2017**, *29* (16), 1605993.
- (7) Hu, X.; Zhang, X.; Liang, L.; Bao, J.; Li, S.; Yang, W.; Xie, Y. High-Performance Flexible Broadband Photodetector Based on Organolead Halide Perovskite. *Adv. Funct. Mater.* **2014**, *24* (46), 7373-7380.

(8) Lian, Z.; Yan, Q.; Lv, Q.; Wang, Y.; Liu, L.; Zhang, L.; Pan, S.; Li, Q.; Wang, L.; Sun, J. L. High-Performance Planar-Type Photodetector on (100) Facet of MAPbI₃ Single Crystal. *Sci. Rep.* **2015**, *5*, 16563.

(9) Waleed, A.; Tavakoli, M. M.; Gu, L.; Wang, Z.; Zhang, D.; Manikandan, A.; Zhang, Q.; Zhang, R.; Chueh, Y. L.; Fan, Z. Lead-Free Perovskite Nanowire Array Photodetectors with Drastically Improved Stability in Nanoengineering Templates. *Nano. Lett.* **2017**, *17* (1), 523-530.

(10) Liu, J.; Xue, Y.; Wang, Z.; Xu, Z. Q.; Zheng, C.; Weber, B.; Song, J.; Wang, Y.; Lu, Y.; Zhang, Y.; Bao, Q. Two-Dimensional CH₃NH₃PbI₃ Perovskite: Synthesis and Optoelectronic Application. *ACS Nano* **2016**, *10* (3), 3536-3542.

(11) Deng, W.; Zhang, X.; Huang, L.; Xu, X.; Wang, L.; Wang, J.; Shang, Q.; Lee, S. T.; Jie, J. Aligned Single-Crystalline Perovskite Microwire Arrays for High-Performance Flexible Image Sensors with Long-Term Stability. *Adv. Mater.* **2016**, *28* (11), 2201-2208.

(12) Hu, Q.; Wu, H.; Sun, J.; Yan, D.; Gao, Y.; Yang, J. Large-area perovskite nanowire arrays fabricated by large-scale roll-to-roll micro-gravure printing and doctor blading. *Nanoscale* **2016**, *8* (9), 5350-5357.

(13) Spina, M.; Bonvin, E.; Sienkiewicz, A.; Nafradi, B.; Forro, L.; Horvath, E. Controlled growth of CH₃NH₃PbI₃ nanowires in arrays of open nanofluidic channels. *Sci. Rep.* **2016**, *6*, 19834.

(14) Zhuo, S.; Zhang, J.; Shi, Y.; Huang, Y.; Zhang, B. Self-template-directed synthesis of porous perovskite nanowires at room temperature for high-performance visible-light photodetectors. *Angew. Chem. Int. Ed.* **2015**, *54* (19), 5693-5696.

- (15) Zhang, F.; Zhong, H.; Chen, C.; Wu, X.; Hu, X.; Huang, H.; Han, J.; Zou, B.; Dong, Y. Brightly Luminescent and Color-Tunable Colloidal $\text{CH}_3\text{NH}_3\text{PbX}_3$ (X = Br, I, Cl) Quantum Dots: Potential Alternatives for Display Technology. *ACS Nano*, **2015**, *9* (4), 4533-4542.
- (16) Fu, R.; Zhao, Y.; Li, Q.; Zhou, W.; Yu, D.; Zhao, Q. Enhanced long-term stability of perovskite solar cells by 3-hydroxypyridine dipping. *Chem. Commun.* **2017**, *53* (11), 1829-1831.
- (17) Wang, Q.; Chen, B.; Liu, Y.; Deng, Y.; Bai, Y.; Dong, Q.; Huang, J. Scaling behavior of moisture-induced grain degradation in polycrystalline hybrid perovskite thin films. *Energy Environ. Sci.* **2017**, *10* (2), 516-522.
- (18) Yun, J. S.; Ho-Baillie, A.; Huang, S.; Woo, S. H.; Heo, Y.; Seidel, J.; Huang, F.; Cheng, Y. B.; Green, M. A. Benefit of Grain Boundaries in Organic-Inorganic Halide Planar Perovskite Solar Cells. *J. Phys. Chem. Lett.* **2015**, *6* (5), 875-880.
- (19) Noel, N. K.; Abate, A.; Stranks, S. D.; Parrott, E. S.; Burlakov, V. M.; Goriely, A.; Snaith, H. J. Enhanced photoluminescence and solar cell performance via Lewis base passivation of organic-inorganic lead halide perovskites. *ACS Nano* **2014**, *8* (10), 9815-9821.
- (20) Lee, J. W.; Kim, H. S.; Park, N. G. Lewis Acid-Base Adduct Approach for High Efficiency Perovskite Solar Cells. *Acc. Chem. Res.* **2016**, *49* (2), 311-319.
- (21) Wang, F.; Geng, W.; Zhou, Y.; Fang, H. H.; Tong, C. J.; Loi, M. A.; Liu, L. M.; Zhao, N. Phenylalkylamine Passivation of Organolead Halide Perovskites Enabling High-Efficiency and Air-Stable Photovoltaic Cells. *Adv. Mater.* **2016**, *28* (45), 9986-9992.

(22) Gao, L.; Zeng, K.; Guo, J.; Ge, C.; Du, J.; Zhao, Y.; Chen, C.; Deng, H.; He, Y.; Song, H.; Niu, G.; Tang, J. Passivated Single-Crystalline CH₃NH₃PbI₃ Nanowire Photodetector with High Detectivity and Polarization Sensitivity. *Nano. Lett.* **2016**, *16* (12), 7446-7454.

(23) Zuo, L.; Guo, H.; Quillettes, D. W.; Jariwala, S.; Marco, N.; Dong, S.; Block, R.; Ginger, D. S.; Dunn, B.; Wang, M.; Yang Y. Polymer-modified halide perovskite films for efficient and stable planar heterojunction solar cells. *Sci. Adv.* **2017**, *3* (8), e1700106.

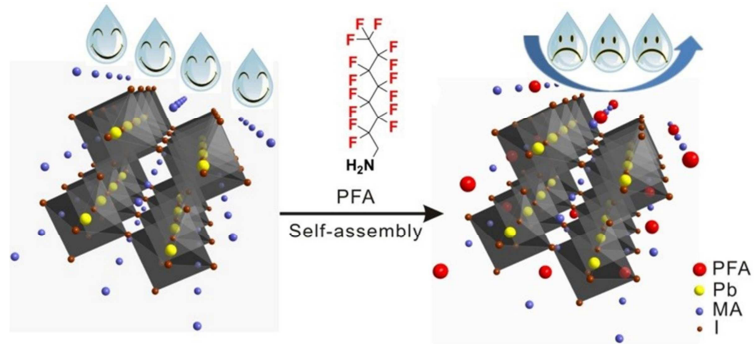
(24) Brivio, F.; Walker, A. B.; Walsh, A. Structural and electronic properties of hybrid perovskites for high-efficiency thin-film photovoltaics from first-principles. *APL Materials* **2013**, *1* (4), 042111.

(25) Dong, D.; Deng, H.; Hu, C.; Song, H.; Qiao, K.; Yang, X.; Zhang, J.; Cai, F.; Tang, J.; Song, H. Bandgap tunable Cs_x(CH₃NH₃)_{1-x}PbI₃ perovskite nanowires by aqueous solution synthesis for optoelectronic devices. *Nanoscale* **2017**, *9* (4), 1567-1574.

(26) Zhu, C.; Tang, Y.; Chen, F.; Manohari, A. G.; Zhu, Y.; Shi, Z.; Xu, C. Fabrication of self-assembly polycrystalline perovskite microwires and photodetectors. *J. Cryst. Growth*, **2016**, *454*, 121-127.

(27) Deng, H.; Dong, D.; Qiao, K.; Bu, L.; Li, B.; Yang, D.; Wang, H. E.; Cheng, Y.; Zhao, Z.; Tang, J.; Song, H. Growth, patterning and alignment of organolead iodide perovskite nanowires for optoelectronic devices. *Nanoscale* **2015**, *7* (9), 4163-4170.

Graphic Abstract



A Novel Passivation Molecule of PFA has Been Adopted for Improving the Optoelectronic Performance and Moisture Stability of the Photodetector Based on 1D Perovskite Microwires.